Iranian Journal of Numerical Analysis and Optimization
Vol. 13, No. 2, 2023, pp 187–204
https://doi.org/10.22067/ijnao.2022.76010.1123
https://ijnao.um.ac.ir/

How to cite this article
Research Article

Approximate solutions to the Allen–Cahn equation using rational radial basis functions method

M. Shiralizadeh*, A. Alipanah and M. Mohammadi

Abstract

We apply the rational radial basis functions (RRBFs) method to solve the Allen–Cahn (A.C) equation, particularly when the equation has a solution with steep front or sharp gradients. We approximate the spatial derivatives by the RRBFs method. Then we apply an explicit, fourth-order Runge–Kutta method to advance the resulting semi-discrete system in time. It is well known that the A.C equation has a nonlinear stability feature, meaning that the free-energy functional is reduced by time. The presented method maintains the total energy reduction property of the A.C equation. In the end, five examples to confirm the efficiency and accuracy of the proposed method are provided.

AMS subject classifications (2020): 65N99, 74G15, 97N40.

Keywords: Allen–Cahn equation, RBFs, Rational RBFs method, Runge–Kutta method.

---

*Corresponding author

Received 4 April 2022; revised 26 July 2022; accepted 26 August 2022

Mansour Shiralizadeh
Department of Applied Mathematics, University of Kurdistan, Sanandaj, Iran.
Department of Mathematics, Payame Noor University (PNU), Tehran, Iran. e-mail: m.shiralizadeh@pnu.ac.ir

Amjad Alipanah
Department of Applied Mathematics, University of Kurdistan, Sanandaj, Iran. e-mail: a.alipanah@uok.ac.ir

Maryam Mohammadi
Faculty of Mathematical Sciences and Computer, Kharazmi University, Tehran, Iran. e-mail: m.mohammadi@khu.ac.ir

1 Introduction

In this paper, we examine the Allen–Cahn (A.C) equation as follows:

$$w_t = \nu w_{zz} - h(w), \qquad z \in [a,b],\ t \in (0,T], \tag{1}$$

with the initial condition

$$w(z,0) = g(z), \qquad z \in [a,b], \tag{2}$$

and Dirichlet boundary conditions as

$$w(a,t) = l(t), \qquad w(b,t) = k(t), \qquad t \in [0,T], \tag{3}$$

where the parameter ν is a positive constant and usually represents the interfacial width. The term $h(w) = H^{'}(w)$ with $H(w) = \frac{1}{4}(w^2-1)^2$ is a given energy potential.

The A.C equation was initially given by Allen and Cahn [1] to illustrate the motion of anti-phase boundaries in crystal solids. The A.C equation is a specific type of nonlinear partial differential equation used extensively to model various phenomena, such as crystal growth [3, 12], phase transitions [6, 28], image analysis [2, 8, 20, 26], texture growth [9, 23, 24, 27], and surface dynamics in material science [13, 21].

We know that the solution $w(z,t)$ to the A.C equation has the feature that the total energy $E_T(w)$ is reduced over time, and it is given as follows:

$$E_T(w) = \int_a^b \left(\tfrac{1}{2}\nu|w_z|^2 + H(w)\right) dz, \tag{4}$$

and may be used to assess the accuracy of the rational radial basis functions (RRBFs) method presented here.

In general, the analytical solution of the A.C equation is not available. So many researchers tend to use numerical methods, such as finite difference [22], finite element [11], Fourier spectral with periodic boundary condition [25], and radial basis functions (RBFs) methods [29]. In recent years, researchers have been interested in developing numerical methods that can preserve the energy dissipation property of the A.C equations.

Among these methods, the meshless technique avoids mesh generation. It uses scattered points instead of meshing the domain of the problem. For more description, see [14, 15, 16, 30, 36, 38]. The RBFs methods are substantial instruments for scattered points interpolation and solving partial differential equations (PDEs). When the underlying function or the solution of PDE is sufficiently smooth, RBFs methods can produce exponential accuracy, but if the underlying function or the solution of PDE has steep gradients or discontinuities, then the RBFs method may produce solutions with oscillation. In such situations, the RRBFs method can be used to approximate derivatives of functions and to solve PDEs [35]. RRBFs method approximating solutions in

nonlinear spaces generated by RBFs is more computationally expensive than the standard RBFs methods. For smooth problems, the accuracy obtained from these methods may not be worth the additional computations. However, for problems with discontinuities and steep fronts, these methods will be considerably more accurate, and the additional computations will be justified.

In 2009, the RRBFs method was used to interpolate functions with steep gradients by Jakobsson, Andersson, and Edelvik [17]. Sarra and Bai [35] extended the method of Jakobsson et al. to interpolate discontinuous functions and solve Burger's equation. The RRBFs-based partition of unity interpolation was used by De Marchi, Martinez, and Perracchione [4], and in [37], the authors used the RRBFs method for solving the Sine-Gordon equation.

In this paper, we apply the RRBFs method for solving (1) with conditions given in (2)–(3), particularly when the equation has a solution with steep front or sharp gradients. We approximate the spatial derivatives by the RRBFs method. Then we apply an explicit, fourth-order Runge–Kutta (RK4) method to advance the resulting semi-discrete system in time.

This paper is organized as follows: In Section 2, we introduce the RBFs and RRBFs methods. The method implementation is given in Section 3. We analyze stability issues in Section 4. In Section 5, we present the results of numerical examples. Section 6 is dedicated to the conclusion.

2 RBFs and Rational RBFs interpolation

2.1 RBFs interpolation

Let $\Gamma \subseteq \mathbb{R}^m$ be a bounded set, let $Z = \{\boldsymbol{z}_1^c, \ldots, \boldsymbol{z}_N^c\} \subseteq \Gamma$ be a set of N distinct points, hereinafter referred to as centers, and let $F = \{f(\boldsymbol{z}_1^c), \ldots, f(\boldsymbol{z}_N^c)\}$ be a set of function values. An RBF

$$\psi(\boldsymbol{z}) = \psi\left(\|\boldsymbol{z} - \boldsymbol{z}^c\|_2, \epsilon\right), \qquad \boldsymbol{z}, \boldsymbol{z}^c \in \mathbb{R}^m,$$

is a function of one variable $r = \|\boldsymbol{z} - \boldsymbol{z}^c\|_2$ that is centered at $\boldsymbol{z}^c$, which ϵ is a free parameter and called the shape parameter [10, 35]. Also, in this paper, $m = 1$.

The inverse quadratic RBF

$$\psi(r) = \frac{1}{1 + (\epsilon r)^2}$$

is a strictly positive definite RBF that we use it in all examples.

The RBF interpolant takes the form

$$p(\boldsymbol{z}) = \sum_{j=1}^{N} c_j \ \psi\left(\|\boldsymbol{z} - \boldsymbol{z}_j^c\|_2 \, , \, \epsilon\right), \tag{5}$$

which the coefficients c_j are obtained by solving the linear system

$$A\mathbf{c} = \mathbf{f},$$

based on the interpolation conditions $p\left(\boldsymbol{z}_i^c\right) = f_i$, where $\mathbf{f} = [f(\boldsymbol{z}_1^c), \ldots, f(\boldsymbol{z}_N^c)]^T$. The elements of the matrix A are of the form

$$a_{ij} = \psi\left(\|\boldsymbol{z}_i^c - \boldsymbol{z}_j^c\|_2 \, , \, \epsilon\right), \qquad i, j = 1, \ldots, N. \tag{6}$$

Moreover, A is a symmetric positive definite matrix and thus invertible. The evaluation of the interpolant (5) at M points $\boldsymbol{z}_j$ is done by multiplying $\mathbf{c}$ by E, where the elements of the matrix E are of the form

$$e_{ij} = \psi\left(\|\boldsymbol{z}_i - \boldsymbol{z}_j^c\|_2 \, , \, \epsilon\right), \qquad i = 1, \ldots, M, \quad j = 1, 2, \ldots, N. \tag{7}$$

The first and second derivatives of RBF interpolant are of the form

$$D(p(\boldsymbol{z})) = \sum_{j=1}^{N} c_j \ D\left(\psi\left(\|\boldsymbol{z} - \boldsymbol{z}_j^c\|_2 \, , \, \epsilon\right)\right).$$

Thus

$$D(p(\boldsymbol{z}_i^c)) = \sum_{j=1}^{N} c_j \ D\psi\left(\|\boldsymbol{z}_i^c - \boldsymbol{z}_j^c\|_2 \, , \, \epsilon\right),$$

that is,

$$D\mathbf{f} \simeq E_D\mathbf{c},$$

where the elements of E_D are of the form

$$(E_D)_{ij} = D\psi\left(\|\boldsymbol{z}_i^c - \boldsymbol{z}_j^c\|_2 \, , \, \epsilon\right), \qquad i, j = 1, \ldots, N,$$

and

$$D(D(p(\boldsymbol{z}))) = \sum_{j=1}^{N} c_j \ D\left(D\psi\left(\|\boldsymbol{z} - \boldsymbol{z}_j^c\|_2 \, , \, \epsilon\right)\right).$$

Thus

$$D(D(p(\boldsymbol{z}_i^c))) = \sum_{j=1}^{N} c_j \ D\left(D\psi\left(\|\boldsymbol{z}_i^c - \boldsymbol{z}_j^c\|_2 \, , \, \epsilon\right)\right),$$

that is,

$$D(D\mathbf{f}) \simeq E_{DD}\mathbf{c},$$

where the elements of E_{DD} are of the form

$$(E_{DD})_{ij} = D\left(D\psi\left(\|\boldsymbol{z}_i^c - \boldsymbol{z}_j^c\|_2\,,\,\epsilon\right)\right), \qquad i,j = 1,\ldots,N.$$

The following theorem [4] gives an error bound in terms of the power function $P_{\psi,Z}$, where $\mathcal{N}_\psi(\Gamma)$ is the native reproducing kernel Hilbert space corresponding to the symmetric positive definite RBF [10].

Theorem 1. Let $\psi \in C(\Gamma \times \Gamma)$ be a strictly positive definite RBF, and suppose that $Z = \{\boldsymbol{z}_1^c,\ldots,\boldsymbol{z}_N^c\} \subseteq \Gamma$ is a set of distinct points and that p is the interpolant to $f \in \mathcal{N}_\psi(\Gamma)$. Then for all $\boldsymbol{z} \in \Gamma$, we have

$$|f(\boldsymbol{z}) - p(\boldsymbol{z})| \leq P_{\psi,Z}(\boldsymbol{z})\|f\|_{\mathcal{N}_{\psi(\Gamma)}}.$$

2.2 Rational RBFs interpolation

The RBFs interpolants have problems, such as ill-conditioning, especially when the shape parameter tends to zero. These problems might lead to inaccurate solutions, particularly when the functions with steep front or sharp gradients are considered [33]. Moreover, when the functions have steep fronts or sharp gradients, the rational RBFs method approximates them better than the standard RBFs method [35]. These are the main reasons that we use rational RBFs interpolants.

The RRBF interpolant of function f is given by

$$\mathcal{Q}(\boldsymbol{z}) = \frac{u(\boldsymbol{z})}{v(\boldsymbol{z})},$$

that satisfies in the interpolation conditions

$$\mathcal{Q}(\boldsymbol{z}_k^c) = f(\boldsymbol{z}_k^c), \qquad k = 1,2,\ldots,N,$$

and $u(\boldsymbol{z})$ and $v(\boldsymbol{z})$ are the RBF interpolants

$$u(\boldsymbol{z}) = \sum_{j=1}^{N} c_j^u\ \psi\left(\|\boldsymbol{z} - \boldsymbol{z}_j^c\|_2\,,\,\epsilon\right),$$

and

$$v(\boldsymbol{z}) = \sum_{j=1}^{N} c_j^v\ \psi\left(\|\boldsymbol{z} - \boldsymbol{z}_j^c\|_2\,,\,\epsilon\right).$$

Let $\mathbf{u} = [u(\boldsymbol{z}_1^c),\ldots,u(\boldsymbol{z}_N^c)]^T$ and $\mathbf{v} = [v(\boldsymbol{z}_1^c),\ldots,v(\boldsymbol{z}_N^c)]^T$. By applying the interpolation conditions, we have a system of equations that is underdetermined. Thus in order for the rational interpolant to be defined uniquely, we add an additional condition (for more descriptions, see [17, 35]), which leads the native space semi-norms [10] of the RBF interpolants $u(\boldsymbol{z})$ and $v(\boldsymbol{z})$ to be

minimized. By adding the condition, we will have a minimization problem with the solution $\mathbf{v}$, which is the eigenvector corresponding to the smallest eigenvalue problem

$$R\mathbf{v} = \lambda\mathbf{v},$$

where

$$R = \operatorname{diag}\left(1/\left(\frac{\mathbf{f}^2}{\|\mathbf{f}\|_2^2}+1\right)\right)\left(\frac{DA^{-1}D}{\|\mathbf{f}\|_2^2}+A^{-1}\right), \tag{8}$$

and A is the RBF system matrix given in (6), $\mathbf{f} = [f(\boldsymbol{z}_1^c),\ldots,f(\boldsymbol{z}_N^c)]^T$, and $D = \operatorname{diag}(f(\boldsymbol{z}_1^c),\ldots,f(\boldsymbol{z}_N^c))$. Moreover, division is elementwise and $\mathbf{f}^2$ is an elementwise squaring of the elements of the vector $\mathbf{f}$. When $\mathbf{v}$ is found, $\mathbf{u}$ is obtained by $\mathbf{u} = D\mathbf{v}$. When $\mathbf{u}$ and $\mathbf{v}$ are found, we obtain the coefficients of the RBF interpolants by solving two linear systems,

$$Ac^u = \mathbf{u} \quad \text{and} \quad Ac^v = \mathbf{v}. \tag{9}$$

Now we evaluate the rational interpolant at M points $\boldsymbol{z}_j$ by

$$\mathbf{Q} = \frac{Ec^u}{Ec^v}, \tag{10}$$

where division is elementwise, E is the RBF evaluation matrix (7), and $\mathbf{Q} = [\mathcal{Q}(\boldsymbol{z}_1),\ldots,\mathcal{Q}(\boldsymbol{z}_M)]^T$.

Now, we calculate the derivatives of the rational interpolant at N points $\boldsymbol{z}_i^c$ by applying quotient rule as below:

$$\mathbf{Q}' = \frac{(Ac^v).(E_Dc^u)-(Ac^u).(E_Dc^v)}{(Ac^v)^2}, \tag{11}$$

$$\mathbf{Q}'' = \frac{2(Ac^u).(E_Dc^v)^2+(Ac^v)^2.(E_{DD}c^u)}{(Ac^v)^3} - \frac{(Ac^v).\Big(2\,(E_Dc^u).(E_Dc^v)+(Ac^u).(E_{DD}c^v)\Big)}{(Ac^v)^3}, \tag{12}$$

where $\mathbf{Q}' = \left[\mathcal{Q}'(\boldsymbol{z}_1^c),\ldots,\mathcal{Q}'(\boldsymbol{z}_N^c)\right]^T$, $\mathbf{Q}'' = \left[\mathcal{Q}''(\boldsymbol{z}_1^c),\ldots,\mathcal{Q}''(\boldsymbol{z}_N^c)\right]^T$, A is the RBF system matrix, and E_D and E_{DD} are the first and second derivatives of evaluation matrix at N points $\boldsymbol{z}_i^c$.

It is concluded from (9) and (10) that the RRBFs interpolant is made by the RBFs interpolation matrix A. Therefore, we are able to provide error bounds for the RRBFs interpolation [4]. For this purpose, we must consider $\mathbf{u}$ and $\mathbf{v}$ as the values obtained by sampling some functions r and $s \in \mathcal{N}_\psi(\Gamma)$, respectively.

Proposition 1. Suppose that $\Gamma \subseteq \mathbb{R}^m$, $\psi \in C(\Gamma\times\Gamma)$ is a strictly positive definite RBF, and let $Z = \{\boldsymbol{z}_1^c, \boldsymbol{z}_2^c, \ldots, \boldsymbol{z}_N^c\} \subseteq \Gamma$ be a set of distinct points

and let $\mathcal{Q}$ be the RRBF interpolant to $f \in \mathcal{N}_\psi(\Gamma)$. Moreover, let us suppose $r, s \in \mathcal{N}_\psi(\Gamma)$. Then for all $\boldsymbol{z} \in \Gamma$, we have

$$|f(\boldsymbol{z}) - \mathcal{Q}(\boldsymbol{z})| \leq \frac{1}{|v(\boldsymbol{z})|} \left(|f(\boldsymbol{z})| \|s\|_{\mathcal{N}_\psi(\Gamma)} + \|r\|_{\mathcal{N}_\psi(\Gamma)} \right) P_{\psi,Z}(\boldsymbol{z}).$$

So Proposition 1 gives the error bound for the RRBFs interpolant in terms of data values and power function, as for the standard RBFs interpolant.

3 RRBFs method for solving A.C equation

Now, we use the RRBFs method to solve the A.C equation. In fact, we develop RRBFs to study the A.C equation with Dirichlet boundary conditions. In our method, we employ the derivatives of the RRBFs to approximate the spatial derivatives. Then we apply an explicit, RK4 method to advance the resulting semi-discrete system in time. In fact, we first approximate the spatial derivatives at N centers $\boldsymbol{z}_i^c$ at time t^n, that is,

$$\mathbf{W}_{zz}(z, t^n) = \left[W_{zz}(\boldsymbol{z}_1^c, t^n), W_{zz}(\boldsymbol{z}_2^c, t^n), \ldots, W_{zz}(\boldsymbol{z}_N^c, t^n) \right]^T,$$

of the A.C equation

$$w_t = \nu w_{zz} - h(w)$$

by the RRBFs method, which is given by computing (12) when

$$\mathbf{W}^n = \left[W(\boldsymbol{z}_1^c, t^n), W(\boldsymbol{z}_2^c, t^n), \ldots, W(\boldsymbol{z}_N^c, t^n) \right]^T,$$

is considered instead of $\mathbf{f}$. This leads to a system of ordinary differential equations of the form

$$\mathbf{W}_t = G(\mathbf{W}, t).$$

Then we apply RK4 method to solve the above system of equations as follows:

$$\begin{aligned}
\mathbf{K}_1 &= \Delta t G(\mathbf{W}^n, t^n), \\
\mathbf{K}_2 &= \Delta t G(\mathbf{W}^n + 0.5k_1, t^n + 0.5\Delta t), \\
\mathbf{K}_3 &= \Delta t G(\mathbf{W}^n + 0.5k_2, t^n + 0.5\Delta t), \\
\mathbf{K}_4 &= \Delta t G(\mathbf{W}^n + k_3, t^n + \Delta t), \\
\mathbf{W}^{n+1} &= \mathbf{W}^n + \tfrac{1}{6}(\mathbf{K}_1 + 2\mathbf{K}_2 + 2\mathbf{K}_3 + \mathbf{K}_4),
\end{aligned} \tag{13}$$

where $t^n = t^{n-1} + \Delta t$ and Δt is the time step size. Clearly, to obtain $\mathbf{W}^1$ initial value, $\mathbf{W}^0$ is required in the iterative computation. Using the initial condition in (2), we have $\mathbf{W}^0 = \left[g(\boldsymbol{z}_1^c), g(\boldsymbol{z}_2^c), \ldots, g(\boldsymbol{z}_N^c) \right]^T$.

To apply the Dirichlet boundary conditions (3), we directly replace $W(\boldsymbol{z}_1^c, t^n)$ with $w(a, t^n) = l(t^n)$ and $W(\boldsymbol{z}_N^c, t^n)$ with $w(b, t^n) = k(t^n)$.

4 Stability issue

Since the RRBFs interpolant is constructed by using the standard RBFs interpolation matrix, the RRBFs method can also suffer from instability problems, especially for $\epsilon \to 0$. In fact, serious problems of ill-conditioning may occur by choosing the wrong values of the shape parameter, particularly for infinitely smooth RBFs. In order for the system matrix B to be well-conditioned, the shape parameter ϵ must not be too small, but small shape parameters are required to obtain better accuracy for the interpolation with RBFs. This is known as the uncertainty principle. We choose the shape parameter ϵ so that the collocation matrix B has a condition number, $\kappa(B)$, in the range $10^{13} \leq \kappa(B) \leq 10^{15}$, in order to determine the proper value for ϵ [34]. These bounds for the condition number are valid when using a computer that implements double precision floating point arithmetic, but the bounds will be different when using other floating point number systems.

5 Numerical results

In this section, we consider five numerical examples of the A.C equation to validate the presented scheme. The accuracy and efficiency of the method are confirmed by calculating L_∞, L_2, and RMS error norms as follows. We also investigate energy dissipation property in our numerical experiments to illustrate the efficiency of the presented method.

$$L_\infty = \|\mathbf{W} - \mathbf{w}\|_\infty,$$

$$L_2 = \|\mathbf{W} - \mathbf{w}\|_2,$$

$$RMS = \sqrt{\tfrac{1}{N}\|\mathbf{W} - \mathbf{w}\|_2},$$

where $\mathbf{w}$ and $\mathbf{W}$ are the exact and numerical solutions, respectively. Moreover, in all numerical examples, we have used uniformly spaced centers

$$\boldsymbol{z}_i^c = a + \frac{i-1}{N-1}(b-a), \qquad i = 1, 2, \ldots, N.$$

Also in the examples, we evaluate the total energy E_T given in (4) using the composite trapezoidal rule for integration.

Example 1. In this example, we examine the A.C equation with three large gradients

$$w_t = \nu w_{zz} + w - w^3, \qquad z \in [-1, 1],$$

and with the initial and Dirichlet boundary conditions [18]

$$w(z, 0) = 0.5z - 0.5\sin(1.5\pi z), \quad w(1, t) = -w(-1, t) = 1.$$

The results are obtained using $\nu = 10^{-5}$, $k = \Delta t = 0.01$, shape parameter $\epsilon = 6$, and $N = 100$ centers. In Figure 1, we present the approximate solution at time $t = 10$ and the space-time graph of the approximate solution. Table 1 shows the values of the energy at various times. It can be seen from Table 1 that energy reduces over time and that the RRBFs method resolves the problem accurately.

Table 1: Energy of the A.C equation for Example 1 at several times.

$Time\,(t)$	$t = 0$	$t = 1$	$t = 2$	$t = 5$	$t = 10$	$t = 20$
$Energy\,(E_T)$	0.3403	0.1941	0.0738	0.0017	7.6908e-04	7.6900e-04

Example 2. In this example, we examine the A.C equation

$$w_t = \nu w_{zz} + w - w^3,$$

in the computational domain $[-1, 1] \times [0, 10]$ with the parameter $\nu = 10^{-6}$. The initial condition is given by [31, 5]

$$w(z, 0) = 0.6z + 0.4\sin\left(\frac{\pi}{2}(z^2 - 3z - 1)\right),$$

and the Dirichlet boundary conditions are

$$w(1, t) = -w(-1, t) = 1.$$

We solve the problem with the RRBFs method with $k = \Delta t = 0.01$, $N = 100$ centers, and the shape parameter $\epsilon = 6$. We have obtained the solution up to time $t = 10$. The graph of approximate solutions at times $t = 0, 2, 4, 6, 10$ and space-time graph for $t \in [4, 10]$ are shown in Figure 2. As it is seen, the solution has a steep front at different times. Table 2 shows the energy at several times. It can be seen from Table 2 that energy reduces over time as theory guarantees and that the RRBFs method resolves the problem accurately.

Example 3. Consider the A.C equation

$$w_t = \nu w_{zz} + w - w^3, \qquad z \in [0, 1], \quad t \geq 0$$

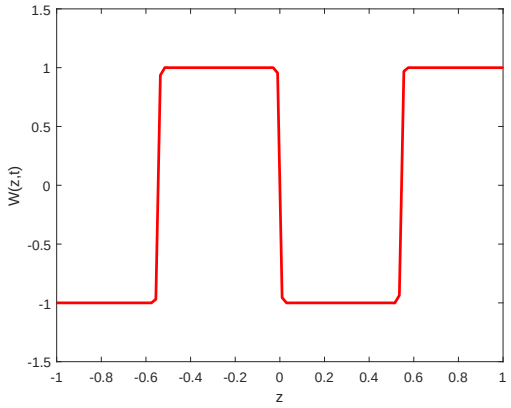

(a) RRBFs solution at time $t = 10$.

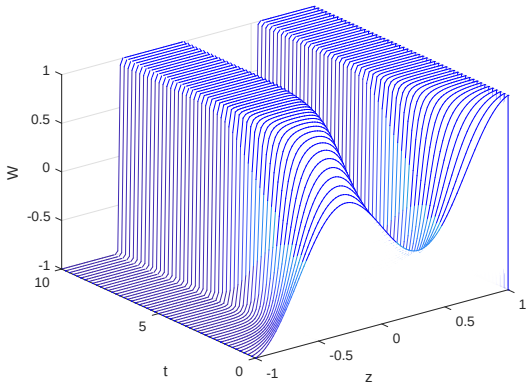

(b) Space-time graph.

Figure 1: Numerical results for the solution of Example 1.

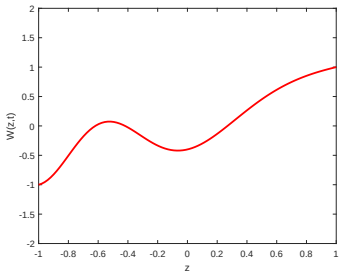

(a) RRBFs solution at time $t = 0$.

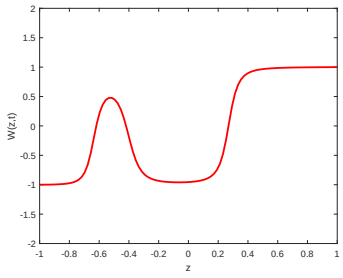

(b) RRBFs solution at time $t = 2$.

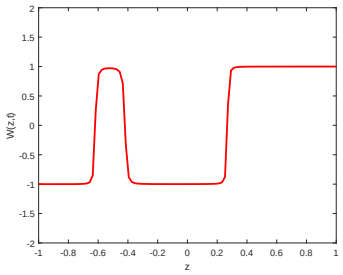

(c) RRBFs solution at time $t = 4$.

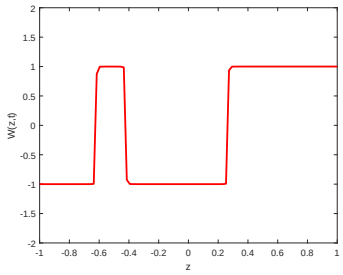

(d) RRBFs solution at time $t = 6$.

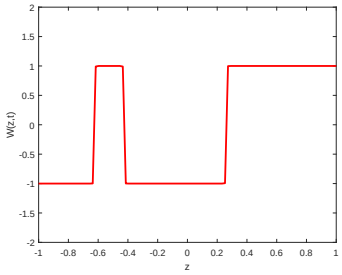

(e) RRBFs solution at time $t = 10$.

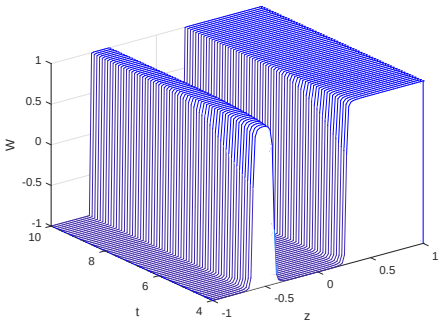

(f) Space-time graph.

Figure 2: Numerical results for the solution of Example 2.

Table 2: Energy of the A.C equation for Example 2 at several times.

$Time\,(t)$	$t=0$	$t=2$	$t=4$	$t=6$	$t=10$
$Energy\,(E_T)$	0.3161	0.0945	0.0154	5.3755e-04	7.1318e-05

with the initial and Dirichlet boundary conditions [7]

$$w(z,0)=\sin(7\pi z),\quad w(0,t)=w(1,t)=0.$$

For the numerical solution, we use $N=100$ centers, $\nu=0.0025$, $k=\Delta t=0.001$, and the shape parameter $\epsilon=8$. The plots of the numerical solution and the energy are shown in Figure 3. It can be seen that energy reduces over time, as the theory guarantees. Compared with [7], better accuracy is obtained.

Example 4. Consider the A.C equation

$$w_t=w_{zz}+\frac{1}{\nu^2}(w-w^3),$$

in the region $0\le z\le 15$, where the parameter $\nu=0.08$, and the initial condition is given by

$$w(z,0)=0.5-0.5\tanh\left(\frac{z-2}{2\sqrt{2}\nu}\right).$$

The analytical solution is given in [19] as

$$w\,(z,t)=0.5-0.5\tanh\left(\frac{z-2-rt}{2\sqrt{2}\nu}\right),$$

where $r=\frac{3}{\sqrt{2}\nu}$, we obtain the Dirichlet boundary conditions from the exact solution and solve this problem with the RRBFs method with $k=\Delta t=0.00001$, $N=200$ centers and the shape parameter $\epsilon=2.25$.

The graphs of exact and approximate solutions at time $t=0.04$ are shown in Figure 4. As it is seen, the solution has a steep front. Table 3 shows the L_∞, L_2, RMS errors, and energy

$$E_T(w)=\int_a^b\left(\frac{1}{2}|w_z|^2+\frac{1}{4\nu^2}(w^2-1)^2\right)dz$$

at several times. It can be seen from Table 3 that the energy reduces over time and that the RRBFs method resolves the problem accurately. Also, the results of the method are well matched with analytical solutions.

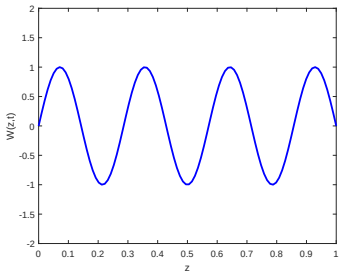

(a) RRBFs solution at time $t = 0$.

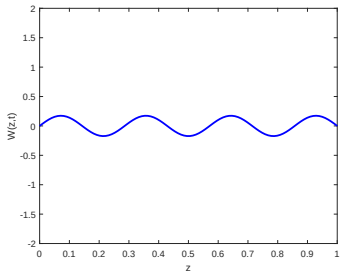

(b) RRBFs solution at time $t = 5$.

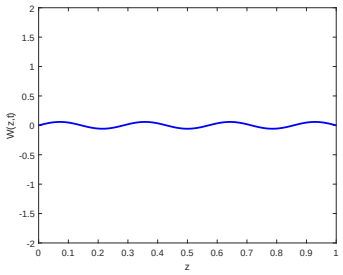

(c) RRBFs solution at time $t = 10$.

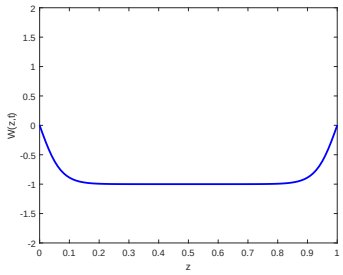

(d) RRBFs solution at time $t = 40$.

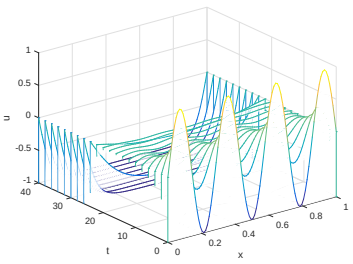

(e) Space-time graph.

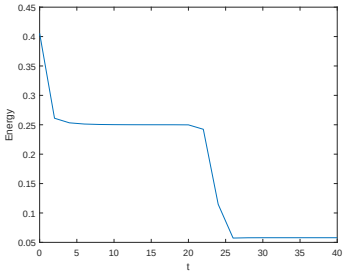

(f) energy evolution.

Figure 3: Numerical results for the solution of Example 3.

Table 3: Errors and energy of Example 4.

t	L_∞	L_2	RMS	$Energy\,(E_T)$
0	0	0	0	509.2856
0.001	2.3112e-05	2.3259e-05	1.6447e-06	508.2498
0.005	5.8036e-04	1.2000e-03	8.2960e-05	504.0963
0.01	5.8573e-04	1.2000e-03	8.2963e-05	498.9173
0.04	7.8661e-05	1.6396e-04	1.1594e-05	467.8536

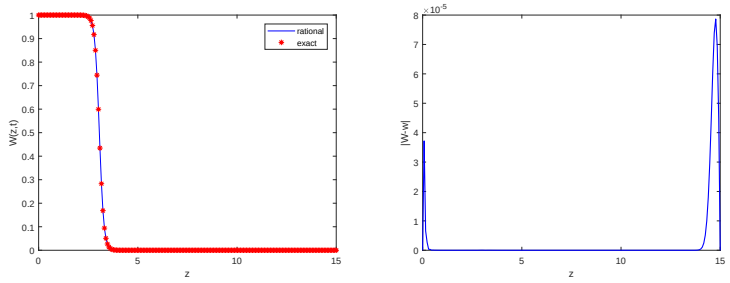

(a) RRBFs and analytical solutions at $t = 0.04$.

(b) Pointwise error at $t = 0.04$.

Figure 4: Numerical results for the solution of Example 4.

Example 5. Consider the A.C equation

$$w_t = w_{zz} + \frac{1}{\nu^2}(w - w^3),$$

with a forcing term h added by imposing analytical solution $w(z,t) = e^{-t}\cos(2\pi z)$ in the domain $0 \le z \le 1$, where the parameter $\nu = 0.1$ [32]. We obtain the Dirichlet boundary conditions from the analytical solution and solve this problem with the RRBFs method with $k = \Delta t = 10^{-4}/8$, $N = 100$ centers and the shape parameter $\epsilon = 8$. The graphs of exact and approximate solutions at time $t = 0.1$ are shown in Figure 5. Table 4 shows the L_∞, L_2, RMS errors, and energy at several times. It can be seen from Table 4 that the energy reduces over time and that the RRBFs method resolves the problem accurately. Also, the results of the method are well matched with analytical solutions and somehow better than the earlier works.

Table 4: Errors and energy of Example 5.

	RRBF				RBF	[32]
t	L_∞	L_2	RMS	E_T	L_∞	L_∞
0	0	0	0	19.2446	0	-
0.001	1.6671e-07	2.6333e-07	2.6333e-08	19.2374	2.1880e-06	-
0.005	1.7437e-07	3.7249e-07	3.7249e-08	19.2095	2.3599e-06	-
0.01	1.7140e-07	4.2040e-07	4.2040e-08	19.1766	2.3762e-06	8.3500e-06
0.1	1.1485e-05	8.0532e-05	8.0532e-06	18.8965	1.2587e-05	6.6300e-05
0.3	4.2165e-05	2.5234e-04	2.5234e-05	19.5199	6.5511e-04	-

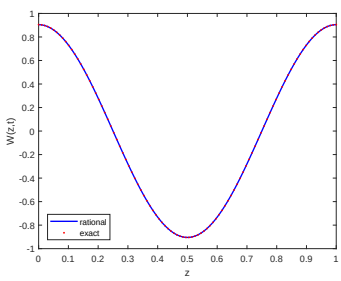

(a) RRBFs and analytical solutions at $t = 0.1$.

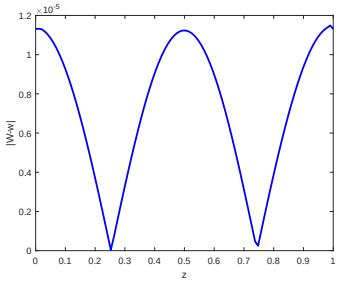

(b) Pointwise error at $t = 0.1$.

Figure 5: Numerical results for the solution of Example 5.

6 Conclusion

This paper investigated the application of the RRBFs method to find the numerical solution of the A.C equation with Dirichlets's boundary conditions, especially when the equation has a solution with steep front or sharp gradients. The combination of RRBFs in space and RK4 in time gave accurate and reliable solutions to the A.C equation. To illustrate the accuracy and efficiency of the presented method, we carried out five examples and presented the corresponding graphs and tables, and compared the results with some earlier works. Moreover, it can be observed that in the case where the analytical solution exists, the numerical solutions described the good accuracy of the method. These results support the assurance of using the method for equation (1) when the analytical solution is not known. In addition, for all examples, the energy dissipation law was investigated. In order to generalize the RRBFs method implementation to higher dimensional time-dependent PDEs, we need to localize the method with a modified partition of the unity method. It is behind the scope of our paper, and we leave it to our further work.

References

[1] Allen, S.M. and Cahn, J.W. *A microscopic theory for antiphase boundary motion and its application to antiphase domain coarsening*, Acta Metall 27 (1979) 1085–1095.

[2] Benes, M., Chalupecky, V. and Mikula, K. *Geometrical image segmentation by the Allen–Cahn equation*, Appl. Numer. Math. 51 (2004) 187–205.

[3] Boettinger, W.J., Warren, J.A., Beckermann, C. and Karma, A. *Phase-field simulation of solidification*, Annu. Rev. Mater. Sci. 32 (2002) 163–194.

[4] De Marchi, S., Martinez, A. and Perracchione, E. *Fast and stable rational RBF-based partition of unity interpolation*, J. Comput. Appl. Math. 349 (2019) 331–343.

[5] Driscoll, A. and Heryudono, R.H. *Adaptive residual subsampling methods for radial basis function interpolation and collocation problems*, Comput. Math. Appl. 53 (2007) 927–939.

[6] Elliott, C.M. and Stinner, B. *Computation of two-phase biomembranes with phase dependent material parameters using surface finite element*, Commun. Comput. Phys. 13 (2013) 325–360.

[7] Elliott, C.M. and Stuart, A.M. *The global dynamics of discrete semilinear parabolic equations*, SIAM J. Numer. Anal. 30 (1993) 1622–1663.

[8] Esedoglu, S. and Tsai, Y.H.R. *Threshold dynamics for the piecewise constant Mumford-Shan functional*, J. Comput. Phys. 211 (2006) 367–384.

[9] Fan, D. and Chen, L.Q. *Computer simulation of grain growth using a continuum field model*, Acta Mater. 45 (1997) 611–622.

[10] Fasshauer, G.E. *Meshfree Approximation Methods with Matlab*, World Scientific, 2007.

[11] Feng, X., Li, Y. and Zhang, Y. *Finite element methods for the stochastics Allen–Cahn equation with gradient-type multiplicative noise*, SIAM J. Numer. Anal. 55(1) (2017) 194–216.

[12] Feng, X., Song, H., Tang, T. and Yang, J. *Nonlinear stability of the implicit-explicit methods for the Allen–Cahn equation*, Inverse Probl. Imaging 7 (2013) 679–695.

[13] Golubovic, L., Levandovsky, A. and Moldovan, D. *Interface dynamics and far-from-equilibrium phase transitions in multilayer epitaxial growth and erosion on crystal surfaces: Continuum theory insights*, East Asian J. Appl. Math. 1 (2011) 297–371.

[14] Heidari, M., Mohammadi, M. and De Marchi, S. *A shape preserving quasi-interpolation operator based on a new transcendental RBF*, Dolomites Research Notes on Approximation 14 (1) (2021) 56–73.

[15] Heydari, M.H. and Hosseininia, M. *A new variable-order fractional derivative with non-singular Mittag-Leffler kernel: application to variable-order fractional version of the 2D Richard equation*, Engineering with Computers 38 (2) (2022) 1759–1770.

[16] Hosseininia, M., Heydari, M.H., Avazzadeh, Z. and Maalek Ghaini, F.M. *A hybrid method based on the orthogonal Bernoulli polynomials and radial basis functions for variable order fractional reaction-advection-diffusion equation*, Engineering Analysis with Boundary Elements 127 (2021) 18–28.

[17] Jakobsson, S., Andersson, B. and Edelvik, F. *Rational radial basis function interpolation with applications to antenna design*, J. Comput. Appl. Math. 233 (2009) 889–904.

[18] Jafari-Varzaneh, H.A. and Hosseini, S.M. *A new map for the Chebyshev pseudospectral solution of differential equations with large gradients*, Numer. Algorithms 69 (2015) 95–108.

[19] Jeong, D. and Kim, J. *An explicit hybrid finite difference scheme for the Allen–Cahn equation*, J. Comput. Appl. Math. 340 (2018) 247–255.

[20] Kay, D.A. and Tomasi, A. *Color image segmentation by the vector valued Allen–Cahn phase-field model: A multigrid solution*, IEEE Trans. Image Process. 18 (2009) 2330–2339.

[21] Kim, J. *Phase-field models for multi-component fluid flows*, Commun. Comput. Phys. 12 (2012) 613–661.

[22] Kim, J., Jeong, D., Yang, S. and Choi, Y. *A finite difference method for a conservative Allen–Cahn equation on non-flat surfaces*, J. Comput. Phys. 334 (2017) 170–181.

[23] Kobayashi, R., Warren, J.A. and Carter, W.C. *A continuum model of grain boundaries*, Phys. D 140 (2000) 141-150.

[24] Krill, C.E. and Chen, L.Q. *Computer simulation of 3-D grain growth using a phase-field model*, Acta Mater. 50 (2002) 3057–3073.

[25] Lee, H. and Lee, J. *A semi-analytical Fourier spectral method for the Allen–Cahn equation*, Comput. Math. Appl. 68 (3) (2014) 174–184.

[26] Lee, H.G., Shin, J. and Lee, J.Y. *First and second order operator splitting method for phase-field crystal equation*, J. Comput. Phys. 299 (2015) 82–91.

[27] Li, Y. and Kim, J. *Multiphase image segmentation using a phase-field model*, Comput. Math. Appl. 62 (2011) 737–745.

[28] Li, Y., Lee, H.G. and Kim, J. A fast, *robust and accurate operator splitting method for Phase-field simulation of crystal growth*, J. Cryst. Growth 321 (2011) 176–182.

[29] Mohammadi, V., Mirzaei, D. and Dehghan, M. *Numerical simulation and error estimation of the time-dependent Allen–Cahn equation on surfaces with radial basis functions*, J. Sci. Comput. 79 (2019) 493–516.

[30] Mohammadi, M., Mokhtari, R. and Schaback, R. *A meshless method for solving the 2d brusselator reaction-diffusion system*, Comput. Model. Eng. Sci. 101 (2014) 113–138.

[31] Naqvi, S.L., Levesley, J. and Ali, S. *Adaptive radial basis function for time dependent partial differential equations*, J. Prime Res. Math. 13 (2017) 90–106.

[32] Niu, J., Xu, M. and Yao, G. *An efficient reproducing kernel method for solving the Allen–Cahn equation*, Appl. Math. Lett. 89 (2019) 78–84.

[33] Perracchione, E. *Rational RBF-based partition of unity method for efficiently and accurately approximating 3D objects*, Comp. Appl. Math. 37 (2018) 4633-4648.

[34] Saberi Zafarghandi, F. and Mohammadi, M. *Numerical approximations for the Riesz space fractional advection-dispersion equations via radial basis functions*, Appl. Numer. Math. 144 (2019) 59–82.

[35] Sarra, S.A. and Bai, Y. *A rational radial basis function method for accurately resolving discontinuities and steep gradients*, Appl. Numer. Math. 130 (2018) 131–142.

[36] Schaback, R. *Kernel-Based Meshless Methods*, Gottingen, 2011.

[37] Shiralizadeh, M., Alipanah, A. and Mohammadi, M. *Numerical solution of one-dimensional Sine-Gordon equation using rational radial basis functions*, J. Math. Model. 10 (3)(2022) 387–405.

[38] Wendland, H. *Scattered data approximation*, Cambridge University Press, 2004.

How to cite this article

, Approximate solutions to the Allen–Cahn equation using rational radial basis functions method. *Iran. j. numer. anal. optim.*, 2023; 13(2): 187-204. https://doi.org/10.22067/ijnao.2022.76010.1123